



Seasonal variations and sources of mass and chemical composition for PM₁₀ aerosol in Hangzhou, China

Junji Cao^{a,b,*}, Zhenxing Shen^b, Judith C. Chow^c, Guowei Qi^d, John G. Watson^c

^a State Key Lab of Loess and Quaternary Geology - SKLLQG, Institute of Earth Environment, Chinese Academy of Sciences, Xi'an, Shaanxi 710075, China

^b Department of Environmental Science and Engineering, Xi'an Jiaotong University, Xi'an 710049, China

^c Division of Atmospheric Sciences, Desert Research Institute, Reno, USA

^d Hangzhou Municipal Environmental Monitoring Center, Hangzhou 310007, China

ARTICLE INFO

Article history:

Received 1 June 2008

Accepted 22 January 2009

Keywords:

PM₁₀
Elements
Ions
Carbon
Material balance

ABSTRACT

Aerosol observation was conducted for four seasons from September 2001 to August 2002 at five sampling sites in Hangzhou, South China, on PM₁₀ mass, 22 elements (Na, Mg, Al, Si, P, S, K, Ca, Ti, V, Cr, Mn, Fe, Ni, Cu, Zn, As, Se, Br, Cd, Ba, and Pb), 5 major ions (F⁻, Cl⁻, NO₃⁻, SO₄²⁻, and NH₄⁺), and organic and elemental carbon (OC and EC), showing that PM₁₀ mass ranged from 46.7 to 270.8 μg/m³, with an annual average of 119.2 μg/m³. Na, Al, Si, S, K, Ca, and Fe were the most abundant elements in PM₁₀, most of S being in the form of SO₄²⁻. SO₄²⁻, NO₃⁻, and NH₄⁺ were the major ions, which contributed to about 20% of the PM₁₀ mass. The mean seasonal concentrations for SO₄²⁻, averaged over all sites, were found to be 18.0, 18.5, 24.7, and 21.4 μg/m³, for spring, summer, autumn, and winter, respectively, while the corresponding loadings for NO₃⁻ were 7.2, 4.7, 7.1, and 11.2 μg/m³, and for NH₄⁺ were 6.0, 5.9, 8.2, and 9.3 μg/m³, in the form mostly of NH₄NO₃ in spring, autumn, and winter, and mostly of (NH₄)₂SO₄ in summer. The low NO₃⁻/SO₄²⁻ ratio found indicates coal combustion as the major source throughout the year. The mean annual concentrations of OC and EC in PM₁₀ were found to be 21.4, and 4.1 μg/m³, respectively. Material balance calculation indicated that fugitive dust, the secondary aerosol, and carbonaceous matter were the most abundant species in PM₁₀ for the four seasons, as is characteristic for cities in South China.

© 2009 Chinese Society of Particuology and Institute of Process Engineering, Chinese Academy of Sciences. Published by Elsevier B.V. All rights reserved.

1. Introduction

The combination of high population density and rapid industrialization in China, especially in the South, has inevitably led to increase in air pollution (e.g., Cao et al., 2003a, 2003b, 2007; Cheng, Ho, Lee, & Law, 2006; Yao et al., 2002; Ye et al., 2003; Yuan, Sau, & Chen, 2004). In addition to deterioration of visibility in urban areas (Watson, 2002), health impact of aerosol has come into view from epidemiological studies associating fine particle concentration to hospital admission records (Harrison & Yin, 2000; Tsai, Apte, & Daisey, 2000). The Chinese government has spared less efforts in establishing stringent emission control strategies. Atmospheric particles with diameters under 10 μm (PM₁₀) are specifically addressed by Air Quality Standards in several nations, since epidemiological evidences suggest that mortality in urban

areas may be linked to PM₁₀ and PM_{2.5} fractions (Dockery et al., 1993; Lundgren & Burton, 1995; Pope, Schwartz, & Ransom, 1992; Schwartz, Dockery, & Neas, 1996). Generally, the total daily mortality increases by approximately 1% for every 10 μg/m³ increase in PM₁₀ concentration (Lippmann, 1998). The composition of atmospheric aerosols also provides useful data for evaluating the optical properties of aerosols (Watson, 2002), such as visibility of the lower atmosphere.

Hangzhou (29.25°–30.5°N, 118.34°–120.75°E), capital city of Zhejiang Province in South China, covers an area of 16,596 km² with a population of 6.29 million inhabitants, and is one of the largest cities in the Yangtze Delta Region (YDR) and also one of the most massively industrialized and urbanized regions in South China. Hangzhou experiences a typical sub-tropic climate with mean annual precipitation of 1705.2 mm, abundant in summer (e.g., 283.4 mm during June) and relatively low in winter (e.g., 44.2 mm during December). The annual mean wind speed is 1.7–2.0 m/s with 10–30% calm days (<0.2 m/s). Prevailing wind direction is mainly southerly in summer and northerly in spring. The atmospheric structure is relatively stable, and temperature inversion often occurs in late autumn and winter. Increased PM₁₀ levels

* Corresponding author. Present address: Institute of Earth Environment, Chinese Academy of Sciences, Xi'an 710075, China. Tel.: +86 29 88326488; fax: +86 29 88320456.

E-mail address: cao@loess.llqg.ac.cn (J. Cao).

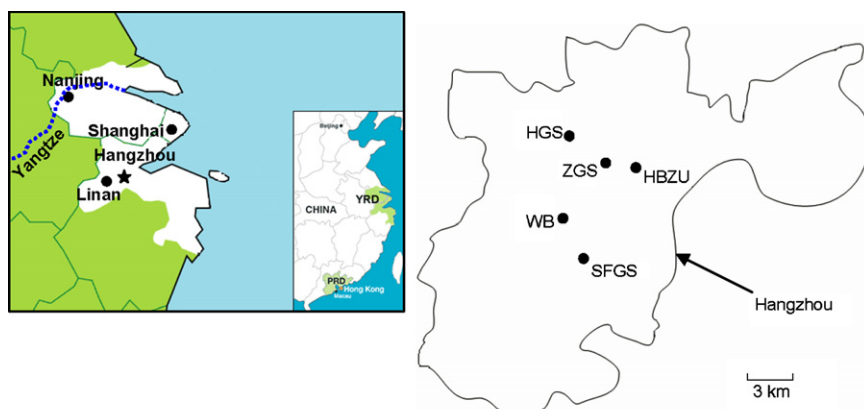


Fig. 1. Location of Hangzhou in Yangtze River Delta of south China and the five sampling sites: HGS: an industrial site; ZGS: a residential site; HBZU: a mixed commercial–residential–traffic site; SFGS: a traffic site; and WB: a background site.

(<http://www.sepa.gov.cn/quality/air.php3>) in Hangzhou have been attributed to the increases in motor vehicles, urban construction, heating installation and industrial combustion, but relatively little data are available on PM_{10} chemical composition. Motor vehicles increased from 0.39 million in 2000 to 1.07 million in 2005. The purpose of this study was to examine spatial and seasonal variations in PM_{10} mass, elemental composition, major water-soluble ions, and carbonaceous species, and to understand the relative contribution of both natural and anthropogenic sources.

2. Methodology

2.1. Sample collection

PM_{10} samples were collected in four seasons from September 2001 to August 2002 at five air quality monitoring stations (Fig. 1): (1) an industrial site in Hemu Grade School (HGS), with three nearby power plants and several factories, (2) a residential site around Zhaohuiwuqu Grade School (ZGS), (3) a mixed commercial–residential–traffic site in Huajiachi Branch of Zhejiang University (HBZU), (4) a traffic site, located near the Second Fux-

ing Grade School (SFGS), and (5) a background site in Wolong Bridge on Xi'shan Road (WB). PM_{10} samples were collected every three days for 24 h duration from 8:00 a.m. PM_{10} samples were collected by an eight-channel automatic cartridge collection unit (ACCU) sampler at ambient temperature combined with the TEOM 1400a (Formerly Rupprecht & Patashnick, currently Thermo Fischer, USA). The ACCU system utilizes the flow splitter and the micro-processor in the TEOM 1400a monitor. The bypass flow is carried to the ACCU system, and then onward to the auxiliary flow controller in the TEOM control unit to ensure a total flow rate of 16.7 L/min through the inlet. If a high-pressure drop occurs and the bypass flow is lower than 13.7 ± 0.4 L/min, the sampling process will be terminated. Only three out of the eight channels are activated simultaneously for each ACCU system using two 47 mm diameter Teflon-membrane filters (Gelman, Ann Arbor, MI) for elemental and water-soluble ionic analyses. The third channel uses 47 mm Whatman quartz microfibre filters (QM/A; Whatman, Middlesex, UK) for the determination of organic and elemental carbon (OC and EC). The quartz filters were pre-heated to 800 °C for 3 h and cooled before use. A total of 176 sets of samples were collected during the study.

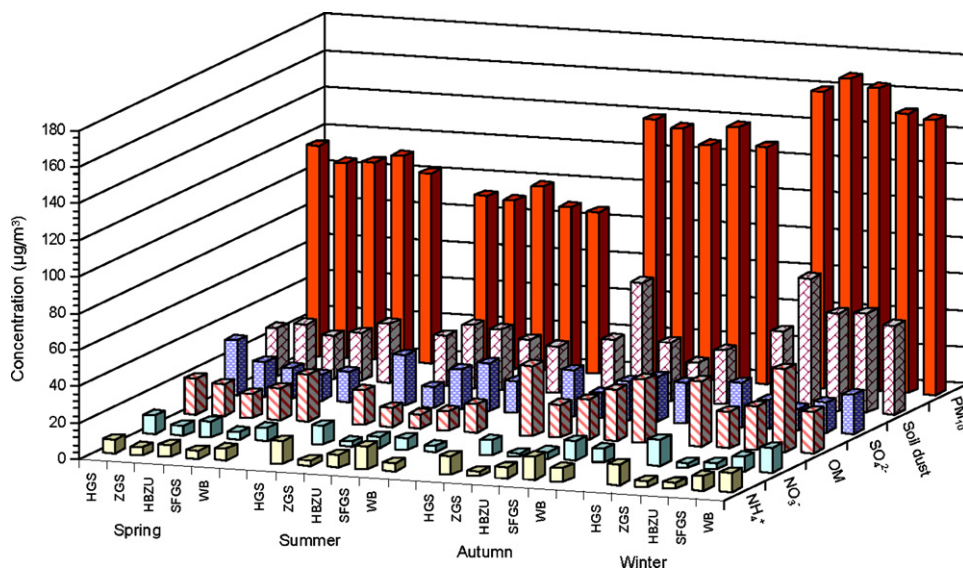


Fig. 2. Seasonal and spatial distributions of PM_{10} mass and major chemical species in Hangzhou: spring (March to May); summer (June to August); autumn (September to November); and winter (December to February).

2.2. Mass and elements analyses

Aerosol mass loadings were determined gravimetrically using a Sartorius MC5 electronic microbalance with a sensitivity of 1 μg . Before weighing, the Teflon filters were equilibrated for a minimum of 24 h at a constant temperature between 20 and 23 $^{\circ}\text{C}$ and relative humidity between 35% and 45%. Each filter was weighed at least three times before and after sampling following the equilibration period. Typical precision for replicate weighing is 10%. The filters were air-tight sealed and preserved in a refrigerator before and after sampling.

Seventeen elements were determined by a proton induced X-ray emission (PIXE, PIXE International Corporation, Tallahassee, FL, USA) method. These elements include Al, Si, P, S, Ca, Ti, V, Cr, Mn, Fe, Ni, Cu, Zn, As, Se, Br, and Pb. These filters were then submitted for acid extraction followed by inductively coupled plasma-atomic emission spectroscopy (ICP-AES, TEIRTA Advantage, USA) for the additional 5 elements (Na, Mg, K, Cd, and Ba).

2.3. Ions analysis

Four anions (F^- , Cl^- , NO_3^- , and SO_4^{2-}) were determined in Teflon filters by an Ion Chromatograph (IC, Dionex 500, Sunnyvale, CA). Prior to analysis, the Teflon filters were placed in 20 mL vials of distilled and deionized water (a resistivity of 18 $\text{M}\Omega$), followed by ultrasonic extraction and mechanical shaking for 1 h each. The extract was stored at 4 $^{\circ}\text{C}$ before analyses. Anions were detected by an AS11-HC column (Dionex Co., Sunnyvale, CA), using 20 mM KOH as the eluent with detection limits less than 0.05 mg/L. Standard Reference Materials produced by the National Research Center for Certified Reference Materials, China, were analyzed for quality assurance purposes. Blank values were subtracted from sample concentrations. Concentration of NH_4^+ was determined by Nessler's reagent colorimetric method.

2.4. Carbonaceous species analysis

The quartz-fiber filters were analyzed, in replicates on 10% of the samples, for OC and EC using a Sunset Model 3 OC/EC Analyzer (Sunset Laboratory Inc., USA) following thermal/optical transmittance (TOT). Eight blank samples were also analyzed and the sample results were corrected by averaging the blank sample concentrations.

3. Results and discussion

3.1. PM_{10} mass concentration

Annual PM_{10} mass concentrations were in the range of 46.7–270.8 $\mu\text{g}/\text{m}^3$, with a five-site arithmetic average and standard deviation (SD) of $119.2 \pm 39.9 \mu\text{g}/\text{m}^3$. This is 20% higher than the annual China ambient air quality PM_{10} Class II standard of 100 $\mu\text{g}/\text{m}^3$. Fig. 2 shows the seasonal and spatial variations of PM_{10} concentrations. The annual average PM_{10} concentration was highest at the industrial HGS site (133 $\mu\text{g}/\text{m}^3$), followed by the traffic-dominated SFGS site (127.8 $\mu\text{g}/\text{m}^3$). Similar annual averages of 112.6 and 114 $\mu\text{g}/\text{m}^3$ were found at the mixed commercial/residential HBZU and background WB sites, respectively. The lowest concentration was found at the residential ZGS site (106.6 $\mu\text{g}/\text{m}^3$). The Chinese air quality Class II standard was exceeded by 1.33 times at the HGS industrial site, 1.27 times at the SFGS traffic site, and 1.1 times at the other sites. High PM_{10} levels at the HGS and SFGS sites suggest the influences of industrial and traffic sources.

PM_{10} mass was highest in winter (with a five-site arithmetic average of 157.2 $\mu\text{g}/\text{m}^3$), followed by autumn (136.8 $\mu\text{g}/\text{m}^3$), with lower concentrations in spring (107.9 $\mu\text{g}/\text{m}^3$) and summer (92.9 $\mu\text{g}/\text{m}^3$). Previous studies showed that about 60–70% of the PM_{10} mass was in the $\text{PM}_{2.5}$ fraction at urban regions (Cao et al., 2003a, 2003b; Ho et al., 2003; Wei et al., 1999). So PM_{10} in Hangzhou was comparable with PM_{10} or $\text{PM}_{2.5}$ data in those cities. Spatial and temporal variations of PM_{10} concentration, shown in Fig. 3, were consistent with the studies on other Chinese cities, such as Beijing (He et al., 2001), Shanghai (Ye et al., 2003), Guangzhou, Shenzhen, Zhuhai and HongKong (Cao et al., 2003a, 2003b), and Nanjing (Wang, Huang, Gao, Gao, & Wang, 2003), which all showed that high PM level occurred in autumn and winter and at industrial and traffic sites.

3.2. Elemental compositions

Table 1 summarizes the annual and seasonal averages of a five-site of PM_{10} mass and chemical components. Most of the elemental concentrations are higher in autumn and winter than in spring and summer. The most abundant PM_{10} elements are Na, Al, Si, S, K, Ca, and Fe, these seven elements accounting for about 24% of PM_{10} mass. High S concentration in PM_{10} was detected, particularly in autumn and winter, which signifies the presence of anthropogenic sources possibly from coal combustion. This can be further supported by comparing the ratios of S/Al between fugitive dust profile samples in the Loess Plateau (Cao et al., 2008) and PM_{10} samples at Hangzhou because there was no fugitive dust profile in Hangzhou. The PM_{10} S/Al ratios were 2.79 in spring, 1.0 in summer, 4.0 in autumn, and 2.5 in winter, which are over three orders of magnitude higher than the S/Al ratio of 0.0056 for fugitive dust profile samples. Seasonal variations of S/Al ratios in Hangzhou were similar to those observed at Xi'an, a typical coal-combustion city in North China (Zhang et al., 2002). PM_{10} Se concentration varied by 2-fold, peaking during autumn ($0.07 \pm 0.04 \mu\text{g}/\text{m}^3$), As concentration was 4–6-fold during winter ($0.31 \pm 0.59 \mu\text{g}/\text{m}^3$), indicative of increasing coal burning during colder seasons. Pb and Br concentrations, markers for vehicle exhaust, are also nearly double during autumn and winter, subsidence inversion during colder seasons may result in the accumulation of vehicle emissions. High Ca concentrations were also observed. The average Ca/Al ratios were 1.25 in spring, 1.65 in summer, 2.16 in autumn, and 1.92 in winter, also much higher than the 0–1 Ca/Al ratio in loess samples (Wen, Diao, & Pan, 1996). As noted in Fig. 3, the variations of Ca/Al ratios are also much higher in autumn and winter as compared to other seasons. The comparison implies that there are non-crustal source contributions to Ca, such as fugitive dust from construction sites or fly ash from coal combustion.

The calculation of enrichment factors relative to earth's upper crust composition can be used to identify the origins of elements from crustal or non-crustal sources (Taylor & McLennan, 1995). The enrichment factors for crustal material (EF_{crust}) were calculated as follows:

$$\text{EF}_{\text{crust}} = \frac{(C_{\text{element}}/C_{\text{reference}})_{\text{air}}}{(C_{\text{element}}/C_{\text{reference}})_{\text{crust}}} \quad (1)$$

where C_{element} is the concentration of any elements, and $C_{\text{reference}}$ is the concentration of the reference element. Typically, Al, Si, Fe, or Ti was chosen as the reference element, of which Ti was used in this study. As shown in Fig. 4, much larger variations were found among elements than among seasons; EF_{crust} for Na, Mg, Al, Si, Ca, and Fe, were in the range of 1–5, indicating that these six elements are mainly from the crustal origin, and the EF_{crust} values for K, V, and Mn were between 5 and 10, implying that these elements were influenced not only by crustal but also by other pollution sources.

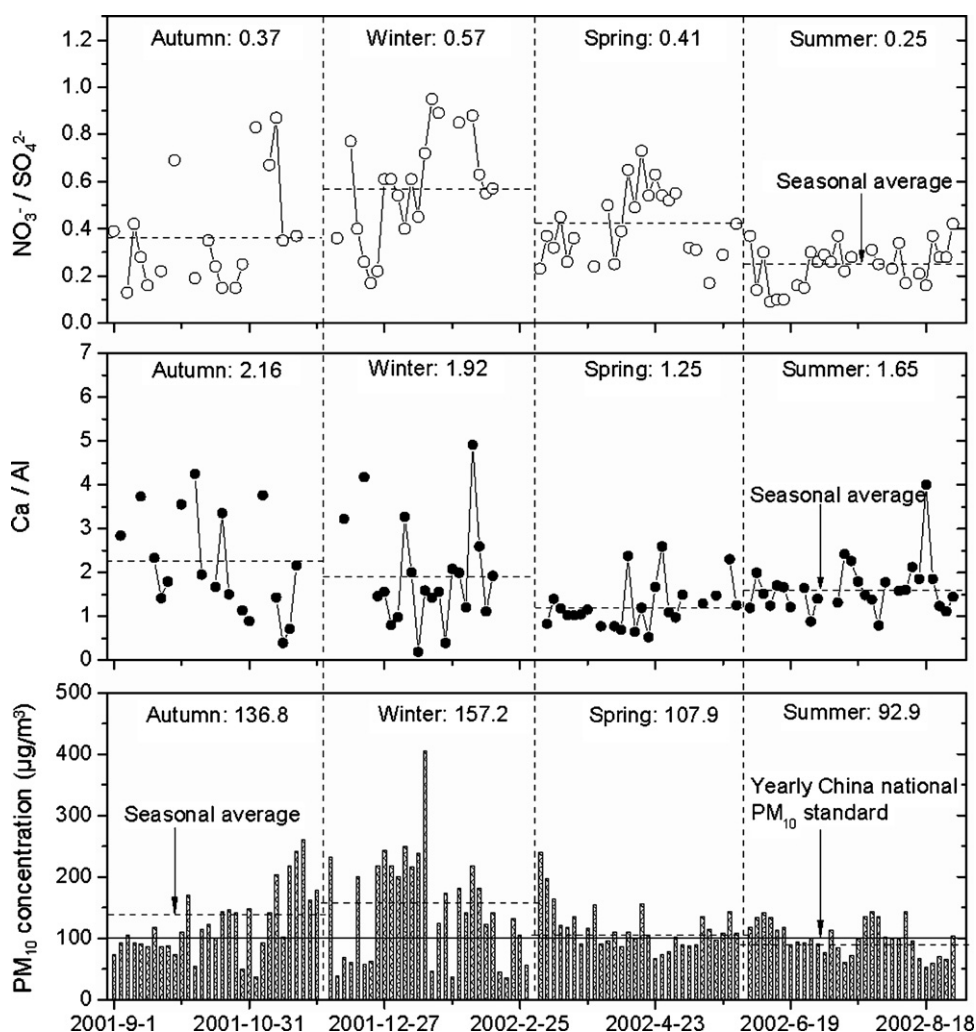


Fig. 3. Temporal variations of 5-site-averages for 24 h PM_{10} mass, Ca/Al ratio, and NO_3^-/SO_4^{2-} ratio at Hangzhou from 9/1/2001 to 8/31/2002. The horizontal dash lines indicate seasonal average values.

For example, EF_{crust} for K was lower than 5 during spring and summer, but increased to around 10 in autumn and winter. In addition to soil dust, an important source for K is biomass burning (Andreae, 1983). Therefore, higher EF_{crust} for K in autumn may imply contribution from biomass burning (such as rice stalks in the harvest season). In contrast, the origins for P, S, Cr, Ni, Cu, Zn, As, Se, Br, Cd, Ba, and Pb were mainly from non-crustal sources due to their much higher EF_{crust} values in the range of 10–1575.

The soil dust mass can be estimated from the concentrations of several indicator elements (Malm, Sisler, Huffman, Eldred, & Cahill, 1994). The following formula, which assumes that the indicator elements occur as their most common oxides, is used in this study:

$$C_{soil} = 2.2C_{Al} + 2.49C_{Si} + 1.63C_{Ca} + 2.42C_{Fe} + 1.94C_{Ti} \quad (2)$$

where C_{soil} is the calculated soil dust concentration, and C_{Al} , C_{Si} , C_{Ca} , C_{Fe} , and C_{Ti} represent the elemental concentrations of Al, Si, Ca, Fe, and Ti in the samples. The average soil dust mass concentrations in PM_{10} were similar in spring ($35.8 \mu\text{g}/\text{m}^3$), summer ($35.3 \mu\text{g}/\text{m}^3$), autumn ($45.4 \mu\text{g}/\text{m}^3$), and winter ($48.9 \mu\text{g}/\text{m}^3$).

3.3. Ionic characteristics

Table 1 lists the annual concentrations for F^- , Cl^- , NO_3^- , SO_4^{2-} , and NH_4^+ in decreasing order: $20.1 \mu\text{g}/\text{m}^3$ (SO_4^{2-}), $7.1 \mu\text{g}/\text{m}^3$

(NO_3^-), $7.0 \mu\text{g}/\text{m}^3$ (NH_4^+), $0.94 \mu\text{g}/\text{m}^3$ (Cl^-), and $0.12 \mu\text{g}/\text{m}^3$ (F^-). The sum of these ions accounts for 33% of PM_{10} mass, indicating that water-soluble ions comprise a large part of aerosol particles. The high SO_4^{2-} concentrations coincide with elevated S in aerosol samples (figure was omitted), with a high correlation coefficient of 0.95 (Sulfate = $2.75 \cdot S + 2.16$, $r = 0.95$, $p < 0.0001$). Annual average ratio of SO_4^{2-}/S was 2.8, close to the value of 3.0 that would be obtained if the entire measured sulfur were oxidized to water-soluble sulphate (Formenti et al., 2003). The present result showed that most of element S was in the form of sulfate in Hangzhou.

The seasonal variations of three major ions, SO_4^{2-} , NO_3^- , and NH_4^+ in Fig. 2, show clear seasonal patterns, e.g., the two peak concentrations of SO_4^{2-} in autumn and winter, decreasing toward spring and summer. Seasonal variations were more pronounced for NO_3^- , with nearly 3-fold increase from summer ($4.7 \pm 4.6 \mu\text{g}/\text{m}^3$) to winter ($11.2 \pm 8.1 \mu\text{g}/\text{m}^3$). NH_4^+ ordered as winter > autumn > spring > summer. The concentrations for Cl^- and F^- had the similar seasonal pattern, in the decreasing order of winter > spring > autumn > summer. The distributions of the major ions in winter and autumn were more scattered than those in summer and spring, implying rather complex sources for these species.

The ratio of NO_3^- to SO_4^{2-} has been used to identify the relative contributions to the aerosol particles from mobile (vehicle exhaust) vs. stationary (coal combustion) sources for S and N in

Table 1
Average ± standard deviation of PM₁₀ mass concentrations at Hangzhou (µg/m³).

	Spring (n = 41) ^a	Summer (n = 59)	Autumn (n = 39)	Winter (n = 38)	Annual (n = 177)
Mass	107.9 ± 27.1	92.9 ± 27.1	136.8 ± 23.3	157.2 ± 43.5	119.2 ± 39.9
Al	2.27 ± 1.29	2.42 ± 1.28	2.34 ± 1.29	4.02 ± 2.67	2.73 ± 1.82
As	0.07 ± 0.06	0.08 ± 0.09	0.05 ± 0.05	0.31 ± 0.59	0.12 ± 0.30
Ba	0.53 ± 0.34	0.30 ± 0.21	0.63 ± 0.69	0.61 ± 0.50	0.48 ± 0.45
Br	0.05 ± 0.07	0.05 ± 0.07	0.08 ± 0.03	0.10 ± 0.05	0.07 ± 0.06
Ca	2.72 ± 2.30	3.91 ± 2.32	4.51 ± 2.06	5.84 ± 2.99	4.17 ± 2.65
Cd	0.01 ± 0.00	0.01 ± 0.01	0.01 ± 0.00	0.01 ± 0.01	0.01 ± 0.01
Cr	0.02 ± 0.02	0.02 ± 0.02	0.02 ± 0.01	0.03 ± 0.02	0.02 ± 0.02
Cu	0.10 ± 0.04	0.13 ± 0.12	0.12 ± 0.06	0.16 ± 0.12	0.13 ± 0.10
Fe	1.92 ± 1.10	2.49 ± 1.51	2.32 ± 1.26	1.92 ± 2.08	2.19 ± 1.54
K	3.26 ± 1.74	3.37 ± 1.74	5.33 ± 2.77	5.37 ± 2.77	4.16 ± 2.42
Mg	0.62 ± 0.41	0.54 ± 0.48	0.47 ± 0.24	0.35 ± 0.23	0.50 ± 0.39
Mn	0.10 ± 0.05	0.11 ± 0.06	0.15 ± 0.09	0.17 ± 0.08	0.13 ± 0.07
Na	0.94 ± 0.82	1.00 ± 1.19	1.26 ± 1.15	1.54 ± 1.46	1.15 ± 1.19
Ni	0.01 ± 0.02	0.01 ± 0.01	0.02 ± 0.03	0.03 ± 0.03	0.02 ± 0.02
P	0.36 ± 0.20	0.53 ± 0.23	0.48 ± 0.35	0.67 ± 0.34	0.51 ± 0.30
Pb	0.25 ± 0.10	0.35 ± 0.24	0.43 ± 0.27	0.49 ± 0.31	0.37 ± 0.25
S	5.16 ± 3.61	4.44 ± 2.65	7.40 ± 2.92	6.98 ± 3.42	5.74 ± 3.34
Se	0.03 ± 0.03	0.03 ± 0.03	0.07 ± 0.04	0.05 ± 0.05	0.04 ± 0.04
Si	8.56 ± 3.74	6.89 ± 3.83	10.83 ± 5.75	10.31 ± 4.04	8.80 ± 4.53
Ti	0.18 ± 0.12	0.20 ± 0.14	0.16 ± 0.16	0.11 ± 0.07	0.17 ± 0.13
V	0.02 ± 0.02	0.02 ± 0.02	0.01 ± 0.02	0.03 ± 0.03	0.02 ± 0.02
Zn	0.34 ± 0.16	0.52 ± 0.32	0.78 ± 0.47	0.65 ± 0.40	0.55 ± 0.37
Cl ⁻	1.00 ± 0.63	0.48 ± 0.43	0.71 ± 0.63	1.87 ± 1.63	0.94 ± 1.02
F ⁻	0.15 ± 0.18	0.07 ± 0.08	0.10 ± 0.09	0.17 ± 0.12	0.12 ± 0.13
NH ₄ ⁺	6.00 ± 3.82	5.87 ± 4.88	8.15 ± 6.89	9.32 ± 5.85	7.03 ± 5.42
NO ₃ ⁻	7.20 ± 5.28	4.68 ± 4.56	7.07 ± 7.05	11.19 ± 8.12	7.12 ± 6.48
SO ₄ ²⁻	15.88 ± 9.51	14.21 ± 7.66	22.81 ± 8.61	21.64 ± 9.90	20.10 ± 12.47
OC	14.03 ± 12.21	13.54 ± 10.23	23.64 ± 21.88	23.81 ± 13.26	21.41 ± 18.03
EC	2.96 ± 2.05	2.82 ± 3.75	4.38 ± 5.49	4.43 ± 2.42	4.06 ± 4.13

^a n: number of samples.

the atmosphere (Arimoto et al., 1996). Kato (1996) reported that gasoline and diesel fuel in China contained 0.12% and 0.2% S (by weight), respectively. The estimated ratios of NO_x to SO_x from the emission of gasoline and diesel fuel burning were 1:8 and 1:13, respectively (Kato, 1996). The S content in coal is around 1% in China and the emission ratio of NO_x to SO_x was 1:2 from coal burning (Wang, Zhuang, Sun, & An, 2005; Yao et al., 2002). Therefore, the low NO₃⁻/SO₄²⁻ ratio could be ascribed to the predominance of stationary source over mobile source pollutions, and vice-versa since oil burning is seldom in Hangzhou. Fig. 3 shows the time series of NO₃⁻/SO₄²⁻ ratios ranging from 0.05 to 1.0, with an annual average of 0.36 ± 0.21. Seasonally, NO₃⁻/SO₄²⁻ ratio showed high values in winter (0.57) and spring (0.41) as compared to those in autumn (0.37) and summer (0.25). Low summer NO₃⁻/SO₄²⁻ ratio (0.25) might be biased because there was nitrate loss when sampling with Teflon in summer. As shown in Fig. 5, the NO₃⁻/SO₄²⁻ ratio in Hangzhou was lower than 0.71 in Beijing (Wang et al., 2005),

0.43 in Shanghai (Yao et al., 2002), and at the same level as 0.35 in Qingdao (Hu et al., 2002), but higher than 0.20 in Taiwan (Fang et al., 2002), and 0.13 in Guiyang (Xiao & Liu, 2004). This annual average NO₃⁻/SO₄²⁻ ratio in urban Hangzhou is also very close to 0.41 in Linan (50 km north of Hangzhou), which represents a background air monitoring station in Yangtze Delta Region, China (Xu et al., 2002). High NO₃⁻/SO₄²⁻ ratios ranging from 2 to 5 were reported by Kim, Teffera and Zeldin (2000) in downtown Los Angeles and in Rubidoux in Southern California, USA, both not using coal. Therefore, the relatively lower NO₃⁻/SO₄²⁻ ratio in Chinese urban cities suggests that stationary emissions (coal combustion) are a dominant source of airborne pollutants in urban atmospheres, as supported by the fact that coal is still the dominant energy source in China.

Table 2 shows the relationships between NH₄⁺ and NO₃⁻, SO₄²⁻, Cl⁻, and F⁻, indicating that NH₄⁺ was closely correlated to NO₃⁻ in summer, autumn, and winter. The slope of the regression between

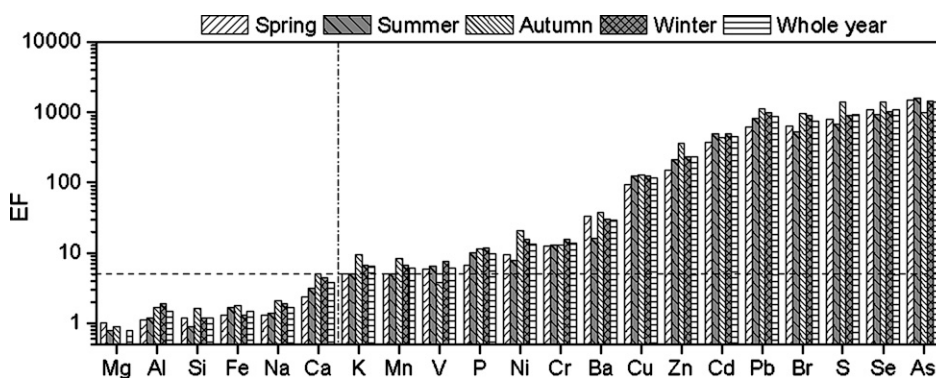


Fig. 4. Enrichment factors (EF) for the 21 elements in four seasons.

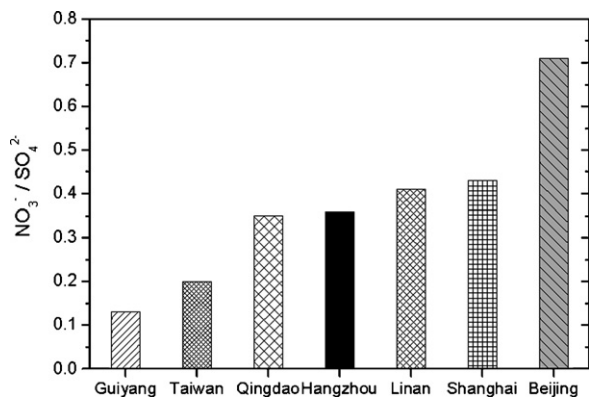


Fig. 5. $\text{NO}_3^-/\text{SO}_4^{2-}$ ratios in different Chinese cities: Beijing (Wang et al., 2005), Shanghai (Yao et al., 2002), Linan (Xu et al., 2002), Hangzhou (this work), Qingdao (Hu et al., 2002), Taiwan (Fang et al., 2002), and Guiyang (Xiao & Liu, 2004).

NH_4^+ and NO_3^- was 0.57 (μg vs. μg) in spring, 0.87 in autumn, and 0.66 in winter. These high slopes indicate that NO_3^- was completely neutralized by NH_4^+ and suggest that NH_4NO_3 was the specie formed by NH_4^+ and NO_3^- in spring, autumn, and winter. The remaining NH_4^+ will then combine with SO_4^{2-} for their relatively lower correlation coefficient. The calculated concentrations of NH_4NO_3 based on NO_3^- concentration were 9.3, 9.1, and $14.4 \mu\text{g}/\text{m}^3$ in spring, autumn, and winter, respectively. The concentration of NO_3^- depends on ambient temperature and relative humidity (RH), which determine the gas-to-particle conversion and partitioning between NO_3^- and HNO_3 (Wastson, Chow, Lurmann, & Musarra, 1994). Lower ambient temperature in winter time favours the formation of NH_4NO_3 as the measured NH_4NO_3 was high in winter. During summer, NH_4^+ was strongly correlated with SO_4^{2-} and NO_3^- with high correlation coefficients of 0.92, and 0.9, respectively. The slope of the regression equation between NH_4^+ and SO_4^{2-} was 0.39, implying that SO_4^{2-} was neutralized completely by NH_4^+ to $(\text{NH}_4)_2\text{SO}_4$ in summer. The remaining NH_4^+ was associated with NO_3^- . If we assumed that SO_4^{2-} was neutralized completely

Table 2
The correlation coefficients (*R*) between major ions and regression equation.

	<i>R</i>	SO_4^{2-}	NO_3^-	Cl^-	F^-	Regression equation	
NH_4^+	Spring (<i>n</i> = 41)	0.66	0.79	0.58	0.2	$\text{NH}_4^+ = 0.26\text{SO}_4^{2-} + 1.28$	$\text{NH}_4^+ = 0.57\text{NO}_3^- + 1.87$
	Summer (<i>n</i> = 59)	0.92	0.90	0.27	0.78	$\text{NH}_4^+ = 0.39\text{SO}_4^{2-} - 1.34$	$\text{NH}_4^+ = 0.97\text{NO}_3^- + 1.31$
	Autumn (<i>n</i> = 39)	0.67	0.89	0.12	0.24	$\text{NH}_4^+ = 0.44\text{SO}_4^{2-} - 0.93$	$\text{NH}_4^+ = 0.87\text{NO}_3^- + 2.0$
	Winter (<i>n</i> = 38)	0.88	0.91	0.66	0.58	$\text{NH}_4^+ = 0.52\text{SO}_4^{2-} - 1.17$	$\text{NH}_4^+ = 0.66\text{NO}_3^- + 1.95$

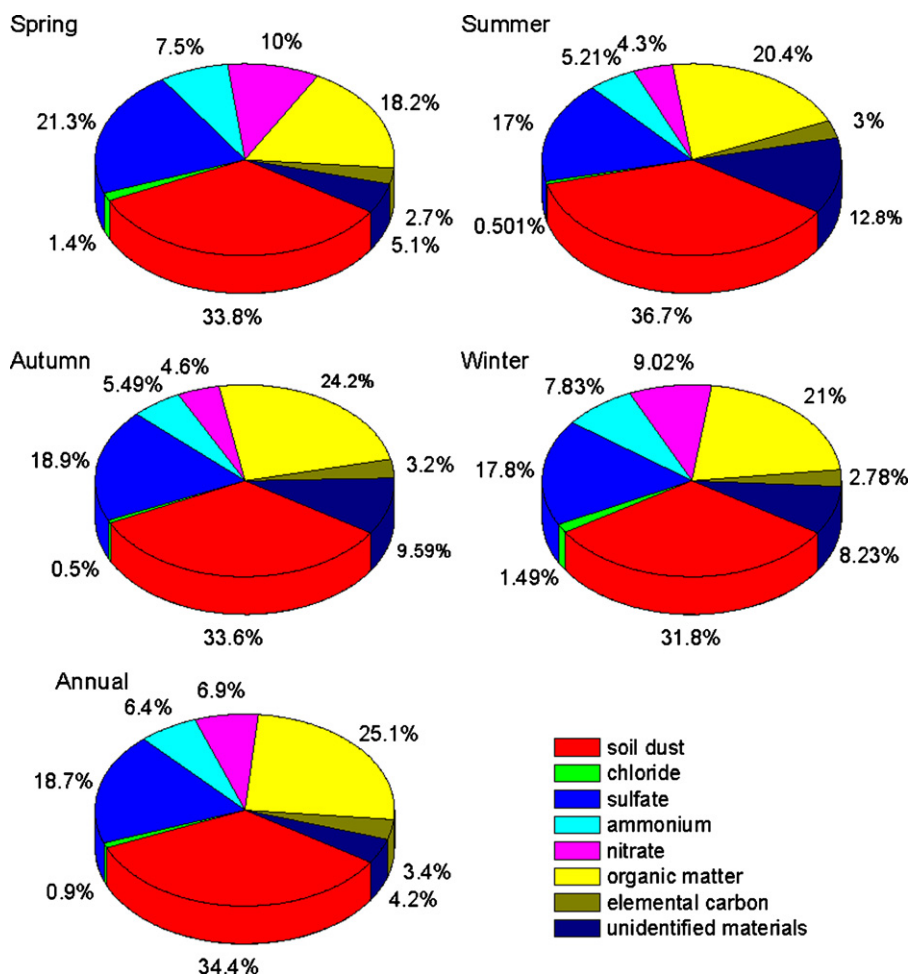


Fig. 6. Material balance of PM_{10} at Hangzhou (soil dust = $2.2C_{\text{Al}} + 2.49C_{\text{Si}} + 1.63C_{\text{Ca}} + 2.42C_{\text{Fe}} + 1.94C_{\text{Ti}}$; OM = 1.4OC).

by NH_4^+ in summer, the concentration of $(\text{NH}_4)_2\text{SO}_4$ can be estimated as $25.4 \mu\text{g}/\text{m}^3$ by using SO_4^{2-} mass level. The much higher correlations between NH_4^+ with NO_3^- and SO_4^{2-} in summer than in other seasons suggest that high temperature, RH (relative humidity), and radiation favoured the formation of secondary aerosols.

3.4. Carbonaceous species

The annual mean concentrations of OC ($21.41 \pm 18.03 \mu\text{g}/\text{m}^3$) and EC ($4.06 \pm 4.13 \mu\text{g}/\text{m}^3$) in PM_{10} at Hangzhou accounted for 18% and 3.4% of PM_{10} mass, respectively. OC and EC had similar seasonal patterns as the major ions as shown in Table 1. High levels of OC and EC observed in autumn and winter were about twice those in spring and summer. The amount of organic matter (OM) in the atmosphere was estimated to be 1.4 times the amount of organic carbon (White & Roberts, 1977). Carbonaceous matter (CM) was calculated as the sum of OM and EC, so that, carbonaceous matter would be $22.6 \mu\text{g}/\text{m}^3$ in spring, $21.8 \mu\text{g}/\text{m}^3$ in summer, $37.5 \mu\text{g}/\text{m}^3$ in autumn, and $37.8 \mu\text{g}/\text{m}^3$ in winter, averaging $34.0 \mu\text{g}/\text{m}^3$ annually, which accounts for 24% of PM_{10} mass.

High correlation ($r = 0.84, p < 0.0005$) was found between OC and EC (figure is omitted), suggesting a common source of carbon (Cao et al., 2003a, 2003b, 2005; Chow et al., 1996; He et al., 2001). Given the large quantities of coal-fired power plants in or near the urban districts and the high concentrations of elements such as S, As, Se, and Zn, as linked to coal combustion (Xu et al., 2003), more contributions from this source are expected.

3.5. Material balance

Fig. 6 shows the relative contributions of major chemical species to PM_{10} . Soil dust accounts for about one-third of annual PM_{10} , which is slightly higher in summer (36.7%), followed by spring (33.8%), autumn (33.6%), and lowest in winter (31.8%). The secondary aerosol was the second most abundant component for each season. During spring, SO_4^{2-} dominated the chemical composition, contributing 21.3% to the PM_{10} , decreasing in the order of autumn (18.9%), winter (17.8%), and summer (17%). The contributions of NO_3^- to PM_{10} decreased from 9–10% during spring and winter to 4.3% and 4.6% during summer and autumn. NH_4^+ follows a similar seasonal pattern as NO_3^- , decreasing from winter (7.8%), spring (7.5%), autumn (5.5%), to summer (5.2%). Carbonaceous matter accounted for 27.4% of the PM_{10} in autumn, followed by winter (23.8%) and summer (23.4%), with the lowest occurring in spring (20.9%). Chloride was considerably less, contributing from 0.5% (summer and autumn) to 1.4% (spring and winter) of PM_{10} . Although Hangzhou is only about 100 km from the East China Sea, the results indicate negligible sea salt influences on PM. Compared to Beijing in northern China (Sun et al., 2006), which was heavily influenced by the eolian dust from the semi-arid and arid region in North China, mineral dust dominated the PM_{10} loading during late autumn in Beijing, which contributed 35–80% of the PM_{10} , with 9% SO_4^{2-} , 6% NO_3^- and 3% NH_4^+ . The high SO_4^{2-} concentration and percentage imply that coal combustion is the most likely major source of pollution particles at Hangzhou.

About 5.1–12.8% of the PM_{10} is unidentified. This may be due to uncertainties in chemical analyses, the assumed mineral oxides, and the use of the multiple 1.4 in OM to account for the hydrogen, nitrogen, and oxygen that are associated with OC.

4. Conclusion

The annual average concentration of PM_{10} in Hangzhou was $119.2 \pm 39.9 \mu\text{g}/\text{m}^3$, which was higher than the annual China National Air Quality PM_{10} Class II Standard of $100 \mu\text{g}/\text{m}^3$. The

seasonal averages of PM_{10} mass concentration were highest in winter, followed by autumn, decreasing in spring, and lowest in summer. Fugitive dust is one of the most abundant components, which accounted for about one-third of annual PM_{10} mass and was mainly from re-suspended road dust or construction soil. Secondary aerosol including SO_4^{2-} , NO_3^- , and NH_4^+ , was the second most abundant component of PM_{10} , contributing between 26.5% and 38.8% of PM_{10} mass in the four seasons. The high SO_4^{2-} concentration and percentage imply that coal combustion is likely an important source of local air pollutants in Hangzhou. This finding was also supported by the relatively lower $\text{NO}_3^-/\text{SO}_4^{2-}$ ratio in this study. Carbonaceous matter was also an important component in PM_{10} , with no apparent difference in the four seasons, ranging from 20.9% to 27.4% in the PM_{10} mass. Therefore, PM_{10} and its detailed chemical species indicate that winter and autumn were heavy pollution seasons in Hangzhou.

Acknowledgement

This work was supported by the National Natural Science Foundation of China (Grants 40675081 and 40599422).

References

- Andreae, M. O. (1983). Soot carbon and excess fine potassium: Long-range transport of combustion-derived aerosols. *Science*, 220, 1148–1151.
- Arimoto, R., Duce, R. A., Savoie, D. L., Prospero, J. M., Talbot, R., Cullen, J. D., et al. (1996). Relationships among aerosol constituents from Asia and the North Pacific during Pem-West A. *Journal of Geophysical Research*, 101, 2011–2023.
- Cao, J. J., Chow, J. C., Watson, J. G., Wu, F., Han, Y. M., Jin, Z. D., et al. (2008). An size-differentiated source profiles for fugitive dust in the Chinese Loess Plateau. *Atmospheric Environment*, 42, 2261–2275.
- Cao, J. J., Lee, S. C., Chow, J. C., Watson, J. G., Ho, K.F., Zhang, R.J., et al. (2007). Spatial and seasonal distributions of carbonaceous aerosols over China. *Journal of Geophysical Research*, 112, D22S11, doi:10.1029/2006JD008205.
- Cao, J. J., Lee, S. C., Ho, K. F., Zhang, X. Y., Zou, S. C., Fung, K., et al. (2003a). Characteristics of carbonaceous aerosol in Pearl River Delta Region China during 2001 Winter Period. *Atmospheric Environment*, 37, 1451–1460.
- Cao, J. J., Lee, S. C., Ho, K. F., Zou, S. C., Zhang, X. Y., & Pan, J. G. (2003b). Spatial and seasonal distributions of atmospheric carbonaceous aerosols in Pearl River Delta region, China. *China Particology*, 1, 33–37.
- Cao, J. J., Wu, F., Chow, J. C., Lee, S. C., Li, Y., Chen, S. W., et al. (2005). Characterization and source apportionment of atmospheric organic and elemental carbon during fall and winter of 2003 in Xi'an China. *Atmospheric Chemistry and Physics*, 5, 3127–3137.
- Cheng, Y., Ho, K. F., Lee, S. C., & Law, S. W. (2006). Seasonal and diurnal variations of PM_{10} , $\text{PM}_{2.5}$, and PM_{10} in the roadside environment of Hong Kong. *China Particology*, 4(6), 312–315.
- Chow, J. C., Watson, J. G., Lu, Z., Lowenthal, D. H., Frazier, C. A., Solomon, P. A., et al. (1996). Descriptive analysis of $\text{PM}_{2.5}$ and PM_{10} at regionally representative locations during SJVAQS/AUSPEX. *Atmospheric Environment*, 30(12), 2079–2112.
- Dockery, D. W., Pope, C. A., Xu, X., Spengler, J. D., Ware, J. H., Fay, M. A., et al. (1993). An association between air pollution and mortality in six US cities. *The New England Journal of Medicine*, 329, 1753–1759.
- Fang, G. C., Chang, C. N., Wu, Y. S., Fu, P. P., Yang, C. J., Chen, C. D., et al. (2002). Ambient suspended particulate matters and related chemical species study in central Taiwan Taichung during 1998–2001. *Atmospheric Environment*, 36, 1921–1928.
- Formenti, P., Elbert, W., Maenhaut, W., Haywood, J., & Andreae, M. O. (2003). Chemical composition of mineral dust aerosol during the Saharan Dust Experiment (SHADE) airborne campaign in the Cape Verde region, September 2000. *Journal of Geophysical Research*, 108(D18), 8576, doi:10.1029/2002JD002648.
- Harrison, R. M., & Yin, J. (2000). Particulate matter in the atmosphere: Which particle properties are important for its effects on health? *Science of the Total Environment*, 249, 85–101.
- He, K. B., Yang, F. M., Ma, Y. L., Zhang, Q., Yao, X. H., Chan, C. K., et al. (2001). The characteristics of $\text{PM}_{2.5}$ in Beijing, China. *Atmospheric Environment*, 35, 4959–4970.
- Ho, K. F., Lee, S. C., Chan, C. K., Yu, J. C., Chow, J. C., & Yao, X. H. (2003). Characterization of chemical species in $\text{PM}_{2.5}$ and PM_{10} aerosols in Hong Kong. *Atmospheric Environment*, 37, 31–39.
- Hu, M., He, L., Zhang, Y., Wang, M., Kim, Y. P., & Moon, K. C. (2002). Seasonal variation of ionic species in fine particles at Qingdao, China. *Atmospheric Environment*, 36, 5853–5859.
- Kato, N. (1996). Analysis of structure of energy consumption and dynamics of emission of atmospheric species related to the global environmental change (SO_x , NO_x , and CO_2) in Asia. *Atmospheric Environment*, 30, 757–785.
- Kim, B. M., Teffera, S., & Zeldin, M. D. (2000). Characterization of $\text{PM}_{2.5}$ and PM_{10} in the South Coast Air Basin of Southern California: Part 1—Spatial variations. *Journal of the Air and Waste Management Association*, 50, 2034–2044.

- Lippmann, M. (1998). The 1997 US EPA standards for particulate matter and ozone. In R. E. Hester & R. M. Harrison (Eds.), *Issues in environmental science and technology* (pp. 75–99). Cambridge: Royal Society of Chemistry.
- Lundgren, D. A., & Burton, R. M. (1995). Effect of particle size distribution on the cut point between fine and coarse ambient mass fraction. *Inhalation Toxicology*, 7, 131–148.
- Malm, W. C., Sisler, J. F., Huffman, D., Eldred, R. A., & Cahill, T. A. (1994). Spatial and seasonal trends in particle concentration and optical extinction in the United States. *Journal of Geophysical Research*, 99(D1), 1347–1370.
- Pope, C. A., III, Schwartz, J., & Ransom, M. (1992). Daily mortality and PM₁₀ pollution in Utah Valley. *Archives of Environmental Health*, 47, 211–217.
- Schwartz, J., Dockery, D. W., & Neas, L. M. (1996). Is daily mortality associated specifically with fine particles? *Journal of the Air and Waste Management Association*, 46, 927–939.
- Sun, Y. L., Zhuang, G. S., Tang, A. H., Wang, Y., & An, Z. S. (2006). Chemical characteristics of PM_{2.5} and PM₁₀ in Haze-Fog episodes in Beijing. *Environmental Science and Technology*, 40, 3148–3155.
- Taylor, S. R., & McLennan, S. M. (1995). The geochemical evolution of the continental crust. *Reviews of Geophysics*, 33, 241–265.
- Tsai, F. C., Apte, M. G., & Daisey, J. M. (2000). An exploratory analysis of the relationship between mortality and the chemical composition of airborne particulate matter. *Inhalation Toxicology*, 12, 121–135.
- Wang, G. H., Huang, L. M., Gao, S. X., Gao, S. T., & Wang, L. C. (2003). Characterization of water-soluble species of PM₁₀ and PM_{2.5} aerosols in urban area in Nanjing, China. *Atmospheric Environment*, 36(8), 1299–1307.
- Wang, Y., Zhuang, G. S., Sun, Y. L., & An, Z. S. (2005). Water-soluble part of the aerosol in the dust storm season—Evidence of the mixing between mineral and pollution aerosols. *Atmospheric Environment*, 39, 7020–7029.
- Watson, J. G., Chow, J. C., Lurmann, F. W., & Musarra, S. (1994). Ammonium nitrate, nitric acid, and ammonia equilibrium in wintertime, Phoenix, Arizona. *Journal of the Air and Waste Management Association*, 44(4), 405–412.
- Watson, J. G. (2002). Visibility: Science and regulation. *Journal of the Air and Waste Management Association*, 52, 628–713.
- Wei, F., Teng, E., Wu, G., Hu, W., Wilson, W. E., Chapman, R. S., et al. (1999). Ambient concentrations and elemental compositions of PM₁₀ and PM_{2.5} in four Chinese cities. *Environmental Science and Technology*, 33, 4188–4193.
- Wen, Q. Z., Diao, G. Y., & Pan, J. Y. (1996). Comparison of average chemical composition of loess in the Loess Plateau with Clark values of crust. *Acta Pedologica Sinica*, 33(3), 225–231.
- White, W. H., & Roberts, P. T. (1977). On the nature and origins of visibility-reducing aerosols in the Los Angeles air basin. *Atmospheric Environment*, 11, 803–812.
- Xiao, H., & Liu, C. (2004). Chemical characteristics of water soluble components in TSP over Guiyang, SW China, 2003. *Atmospheric Environment*, 38, 6297–6306.
- Xu, J., Bergin, M. H., Yu, X., Liu, G., Zhao, T., Carrico, C. M., et al. (2002). Measurements of aerosol chemical, physical and radiative properties in the Yangtze delta region of China. *Atmospheric Environment*, 36, 161–173.
- Xu, M., Yan, R., Zheng, C., Qiao, Y., Han, J., & Sheng, C. (2003). Status of trace element emission in a coal combustion process: A review. *Fuel Processing Technology*, 85, 215–237.
- Ye, B. M., Ji, X. L., Yang, H. Z., Yao, X. H., Chan, C. K., Cadle, S. H., et al. (2003). Concentration and chemical composition of PM_{2.5} in Shanghai for a 1-year period. *Atmospheric Environment*, 37, 499–510.
- Yao, X., Chan, C. K., Fang, M., Cadle, S., Chan, T., Mulawa, P., et al. (2002). The water-soluble ionic composition of PM_{2.5} in Shanghai and Beijing, China. *Atmospheric Environment*, 36, 4223–4234.
- Yuan, C. S., Sau, C. C., & Chen, M. C. (2004). Influence of Asian dusts on the physico-chemical properties of atmospheric aerosols in Taiwan—Using the Pescadore islands as an example. *China Particuology*, 2(4), 144–152.
- Zhang, X. Y., Cao, J. J., Li, L. M., Arimoto, R., Cheng, Y., Huebert, B., et al. (2002). Characterization of atmospheric aerosol over XiAn in the South Margin of the Loess Plateau China. *Atmospheric Environment*, 36, 4189–4199.